Thin Solid Films 603 (2016) 404–407

Contents lists available at ScienceDirect

Thin Solid Films

journal homepage: www.elsevier.com/locate/tsf

Shifting the aluminum nanoparticle plasmon resonance to the visible with SiN and a-Si thin films

Thomas van der Vliet, Marcel Di Vece *

Soft Condensed Matter, Debye Institute for Nanomaterials Science, Utrecht University, P.O. Box 80000, 3508, TA, Utrecht, The Netherlands
Nanophotonics—Physics of Devices, Debye Institute for Nanomaterials Science, Utrecht University, P.O. Box 80000, 3508, TA, Utrecht, The Netherlands

ARTICLE INFO

Article history:
Received 13 October 2015
Received in revised form 14 January 2016
Accepted 27 February 2016
Available online 3 March 2016

Keywords:
Aluminum
Nanoparticle
SiN
a-Si
Optical absorption
Plasmonics

ABSTRACT

Metal nanoparticles have strong optical resonances, which can be used to enhance optical absorption, particularly in thin film solar cells. Most research on these plasmon resonances in the context of solar cells has been performed on gold and silver nanoparticles. As these materials are expensive, alternatives are needed. Aluminum nanoparticles have a plasmon resonance in the UV, but by embedding these particles in silicon nitride or amorphous silicon, the plasmon resonance can be shifted to the visible part of the spectrum. Using a gas aggregation cluster source for the particles and magnetron sputtering for the thin films, aluminum nanoparticles were embedded in silicon nitride and amorphous silicon thin films, which shifted the optical resonance of the metal nanoparticles. The optical absorption of particles embedded in amorphous silicon was not at the expected wavelength, but the results of particles embedded in silicon nitride were in good agreement with FDTD simulations. This work is a next step for cheap plasmonics in solar cells

1. Introduction

Using plasmonic nanostructures in solar cells could contribute to enhanced absorption in the active layer and thereby increase the solar cell efficiency. This can be achieved by the local field enhancement and scattering of plasmonic nanostructures [1–4]. To date, most research focused on noble metals [5,6], which have strong resonances in the visible part of the spectrum and have the advantage of being inert. However, the high price of noble metals makes them unsuitable for commercial solar cells. Although aluminum has its bulk plasmon resonance in the far UV around 150 nm, its plasmon resonance can be shifted, making it a cheap alternative. The plasmon resonance wavelength of aluminum nanoparticles can be shifted towards the visible by selection of size, shape, and configuration [7–12]. This plasmon resonance shift makes the aluminum particles suitable for solar cells. The electron collision frequency at a plasma frequency in the visible in aluminum is in between that of gold and silver [13], which make Ohmic losses acceptable. A theoretical study by Akimov at al. [14] has demonstrated that aluminum particles increases the optical absorption in a-Si:H over a wide wavelength range, better than silver particles. However, light management by plasmonic nanostructures is mainly interesting for thin film solar cells since they have significant transmittance. This thin thickness also restricts the size of the nanoparticles to about 30 nm. When using such small aluminum particles, oxidation can significantly reduce the aluminum metal size or even completely oxidize it. Therefore, covering the small aluminum particles with a protective layer is desirable.

In this work, the plasmon resonance frequency of small aluminum particles is shifted by embedding in a high refractive index dielectric matrix [15]. The polarizability of free electrons, which are on the surface of a metal, is affected by the polarizability of the surrounding medium. Compared to vacuum, with a surrounding dielectric medium, the electrons move slower, hence the shift towards the red. The use of small aluminum particles for solar cells has so far been limited due to strong oxidation, which in this method is prevented as there is no exposure to the ambient during fabrication. The optical absorption of aluminum particles embedded in a-Si and SiN provides clues to the changed plasmonic behavior of these nanoparticles.

2. Experimental

The aluminum nanoparticles were produced by a gas aggregation cluster source (Oxford Applied Research NF-200B [16,17]). The aluminum particles were deposited on glass samples of 1 cm^2 and 2–3 mm thick. The schematic picture is shown in Fig. 1A. High purity Argon gas was used for the plasma to sputter an Aluminum target of 99.99% purity. The glass slide with Aluminum particles was directly moved, continuously in vacuum, to a separate chamber for sputter deposition of a 25 nm thick amorphous silicon or a silicon nitride film. This small thickness ensures that no interference effects can occur above about 200 nm. Considering that the samples were in vacuum ($<10^{-5}$ mbar) during the

* Corresponding author.
E-mail address: m.divece@uu.nl (M. Di Vece).

http://dx.doi.org/10.1016/j.tsf.2016.02.061
0040-6090/

depositions and the short transit time, the particles were not oxidized during this process. Only by exposure to air on purpose for several minutes, the aluminum particles became oxidized before deposition of the cover layer. It is estimated that a layer of 2–5 nm of oxide is formed [14]. This provided a method to inspect the difference between the metal (plasmonic) and (partially) oxidized particle. Aluminum particles were also deposited on a SiN TEM grid, for transmission electron microscopy inspection (Fig. 1B).

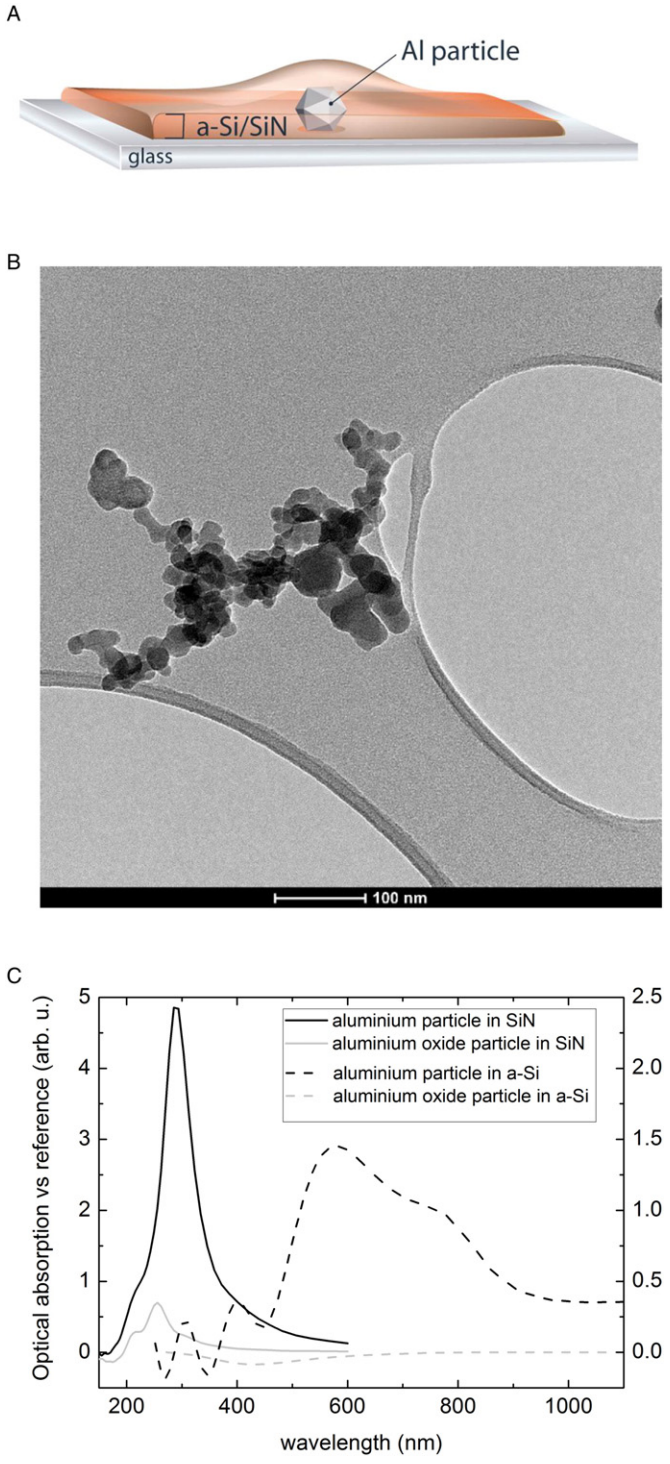

Fig. 1. (A) Schematic depiction of aluminum particles on glass with cover layer. (B) TEM image of aluminum particles, they are merged and oxidized. (C) Simulated optical absorption of aluminum (black) and aluminum particles with an oxide shell (gray) embedded in Si_3N_4 (solid) and a-Si (dashed, right axis).

The particle size and density were inspected with atomic force microscopy (AFM), while the film thickness was determined using the Bruker XT DEKTAK profilometer. The optical absorption measurements were performed with an Agilent Cary 5000 UV–VIS-NIR Spectroscope. The optical absorption spectra of films with particles were compared with films without particles by subtraction. The absorption was calculated by the difference between the reflection and transmission with unity. If the reflection or transmission has a too high value, caused by the limited sensitivity of the setup, the calculated absorption difference can become negative. However, the absorption difference should be positive as the plasmonic aluminium particles can only absorb more light at the plasmon resonance wavelength. Since the spectral properties of the reflection, absorption and transmission are connected through the plasmon resonance the negative value has to be multiplied by −1 to obtain an indication of the proper absorption difference. This method gives a good result for the wavelength dependence of the absorption but only gives an indication of the magnitude of the absorption.

Finite differential time domain (FDTD) simulations were performed with commercial software (Lumerical Solutions, Inc) on spherical particles on glass embedded in a conformal film. A total field scattered field source was used to determine the scattering and absorption cross sections. Convergence was tested for mesh size, simulation setup and boundary layers, which resulted in a 1 or a 1.5 nm mesh size. Pulse lengths are in the order of 2–8 fs. This source is a total field scattered field source which only lets scattered light through its boundaries. This way a field monitor around the source can be used to calculate the scattering cross section of the particle. The boundary conditions are perfectly matched layers (PML), which absorb all the incoming radiation.

3. Results and discussion

The FDTD simulations on aluminum (14 nm) and core (8 nm)-shell (4 nm) aluminum-oxide particles embedded in SiN and a-Si show in Fig. 1C that clear plasmonic resonances are visible at different wavelengths. Aluminum particles of 20 nm size have a plasmon resonance of at about 200 nm (6.2 eV) [7]. The shift of the plasmon resonance to 300 nm (4.1 eV) for SiN and 600 nm (2.1 eV) for a-Si is much larger as compared with plasmon resonance shifts of silver particles in glass and TiO2 [18].

When the particle contains an oxide shell, the plasmon resonance in SiN shifts slightly to 260 nm, which is explained by the lower value of the oxide refractive index around the metal core as compared to an un-oxidized particle. For the particle with oxide shell in a-Si, the plasmon oscillation loses considerable strength and is barely visible, which is likely the result of interband transitions, which are known to dampen plasmon strength [15]. Clearly, the value of the dielectric medium has a strong effect in this wavelength range, which is the onset of an interband transition at 1.4 eV [19]. At a wavelength range between 200 and 600 nm, the value is negative, which indicates that the oxidized aluminum particles transmit or reflect more light. Due to a difference in the absorption coefficient, the plasmonically enhanced local field around the aluminum core will become less absorbed in the aluminum oxide than in a-Si.

The experimentally fabricated aluminum particles embedded in a matrix are investigated with AFM as shown in Fig. 2. The individual particles are visible through the SiN and a-Si cover layer. The lateral features are different because of the tip convolution which differs often per scan. The height of the particles is a measure of their size (plotted in the insets) and has a wide distribution around about 8 nm, depending slightly on each deposition. Considering the conformal growth of the cover layer (matrix) this is a good estimate of the aluminum particle size.

Although the particle density is low, optical absorption spectroscopy provides a measurable effect of the aluminum and oxidized aluminum particles in the order of 1% as shown in Fig. 3. This is also in agreement

with the optical absorption strength as obtained from the FDTD simulations. In Fig. 3, the optical absorption is corrected by the reference layer and particle density. The optical absorption sometimes has a slightly negative values due to an experimental offset because the setup was operated at its limit. However, the aluminum particles in SiN (Fig. 3A) have a clear optical absorption peak at about 350 nm, which is somewhat higher than the 300 nm obtained from the simulations. This is probably the result of a mismatch between the dielectric function used in the simulations and the dielectric function of the experimental SiN film. Although a Si_3N_4 sputter target is used, the stoichiometry and structure of the deposited film can be somewhat different.

The oxidized particles have a clear plasmon resonance at a wavelength of about 370 nm, which is again slightly red shifted as compared with the FDTD simulations due to a different dielectric function of the experimental SiN film. In contrast to the simulation, the optical absorption is similar with respect to the un-oxidized aluminum particles, probably because the oxidation of the aluminum particles is less than expected.

The experimental optical absorption of aluminum particles in a-Si (Fig. 3B) shows that the optical absorption increases from about

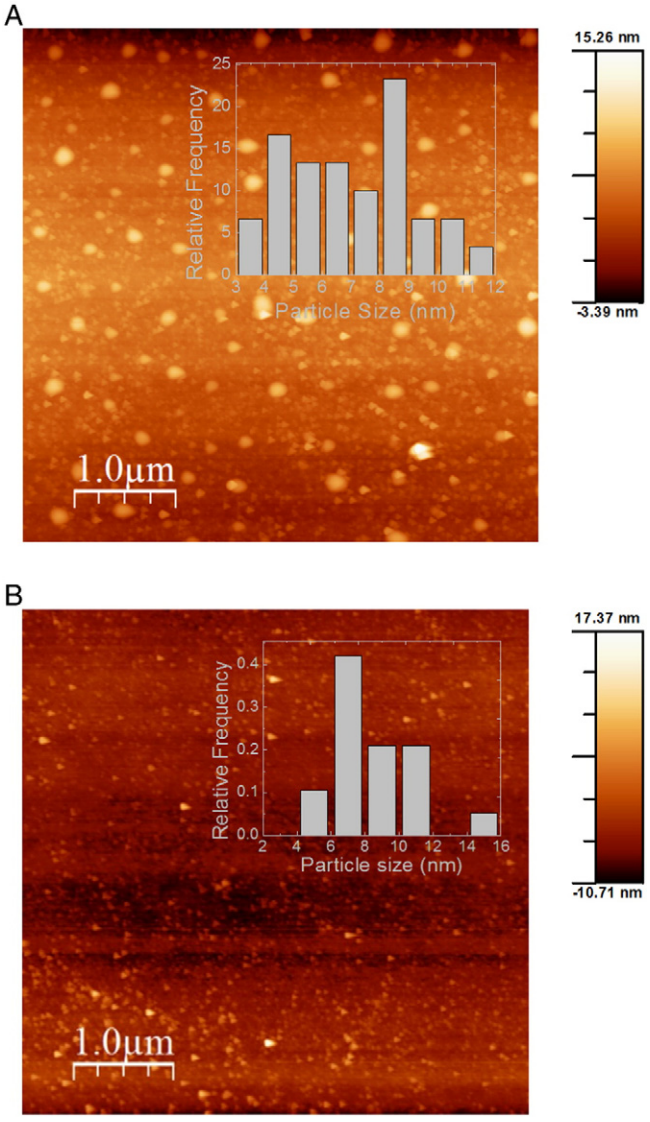

Fig. 2. (A) Aluminum particles on glass covered by a 25 nm Si_3N_4 layer. Features are 5–10 nm in size, which indicates that the Si_3N_4 smoothens some of the roughness underneath. The density is 17 μm^{-2}. (B) 5–10 nm aluminum particles with a 25 nm a-Si layer. The features are 3–12 nm and their density is 7 μm^{-2}.

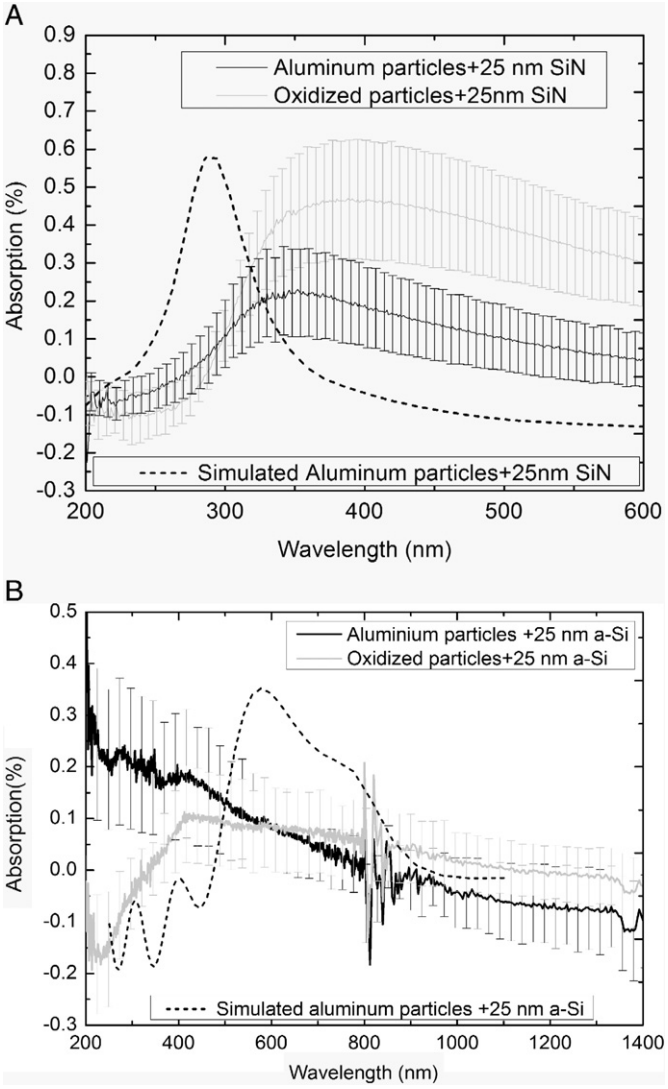

Fig. 3. Optical absorption spectra of aluminum (black) and aluminum particles with an oxide shell (gray) embedded in (A) Si_3N_4 and (B) a-Si. The reference spectrum of the thin film without particles is subtracted and the spectra are corrected for the particle density. The negative values are likely caused by a slight experimental offset. The simulated graphs of Fig. 1C are included (dashed).

1000 nm to lower wavelengths. Because of the error, it is difficult to determine the exact increase. This increase over a broad wavelength range is qualitatively in agreement with the simulations. However, the maximum at about 200 nm is at a much lower wavelength as compared with the simulations (~300 nm). Since the simulations do not predict strong optical absorption between 200 and 400 nm for particles down to 12 nm, this high value of the optical absorption in the blue can be explained by quantum size effects, which considerably blue-shift the plasmon resonance of the smallest particles [20,21]. This effect was not observed in the SiN film because the dielectric value of the matrix determines at which energy quantum confinement effects are active. Due to the strong red shift in a-Si as compared to SiN, it is more pronounced.

The optical absorption of the aluminum-oxide core shell particle in a-Si has an optimum plateau at 500–600 nm. At about 400 nm, the optical absorption decreases considerably. Although the simulations show no measurable peak for the partially oxidized particles, this curve has the same shape as the optical absorption of un-oxidized aluminum particles in a-Si. Again, this indicates that oxidation of the aluminum particles is weaker than expected. However, due to oxidation, the smallest aluminum particles become fully oxidized, removing the possibility for

quantum confinement effects, hence the lower absorption between 200 and 400 nm. The smaller particles with an oxide layer clearly also do not exhibit quantum confinement effects due to the different dielectric environment.

Comparing the aluminum particles in SiN and a-Si leads to the observation that the shift of the plasmon resonance is qualitatively in agreement with their respective dielectric values. Compared to the simulations, the experimental plasmon resonance wavelength is red shifted for the SiN layer, while it is rather blue shifted for the a-Si layer. It is likely that the deposition conditions resulted in thin films with dielectric constants, which were different than the ones used in the simulations.

The optical absorption of the aluminum particles in a-Si and SiN contributes 17% and 2.5% to the total absorption in the wavelength range used. Although the here calculated and measured optical effects of embedding the aluminum nanoparticles in SiN and a-Si are very small (<1% in the measurements), by increasing the particle density, a stronger effect is expected. This would make the here described effects interesting for photovoltaics and other applications.

4. Conclusions

Aluminum nanoparticles are deposited and embedded in SiN and a-Si media by a fast and efficient method using a gas aggregation cluster source combined with thin film deposition. The plasmon resonance wavelength of the aluminum particles in SiN and a-Si was shifted to the visible, although quantum confinement effects resulted in optical absorption in the UV for the a-Si matrix. This effect disappeared upon oxidation of the aluminum particles before the a-Si thin film was deposited. The hereby demonstrated control over the aluminum plasmon resonance by thin film deposition is promising for cheap optical coatings on solar cells and optical sensors.

Acknowledgment

This work has been supported by a Marie Curie Career Integration grant, project no. 293687.

References

[1] S.A. Maier, M.L. Brongersma, P.G. Kik, S. Meltzer, A.A.G. Requicha, H.A. Atwater, Plasmonics—a route to nanoscale optical devices, Adv. Mater. 13 (2001) 1501–1505.
[2] H. Atwater, A. Polman, Plasmonics for improved photovoltaic devices, Nat. Mater. 9 (2009) 205–213.
[3] R.A. Pala, J. White, E. Barnard, J. Liu, M.L. Brongersma, Design of plasmonic thin-film solar cells with broadband absorption enhancements, Adv. Mater. 21 (2009) 3504–3509.
[4] V.E. Ferry, J.N. Munday, H.A. Atwater, Design considerations for plasmonic photovoltaics, Adv. Mater. 22 (2010) 4794–4808.
[5] C. Hägglund, M. Zäch, G. Petersson, B. Kasemo, Enhanced charge carrier generation in dye sensitized solar cells by nanoparticle plasmons, Appl. Phys. Lett. 92 (2008) 053110–053113.
[6] K. Nakayama, K. Tanabe, H.A. Atwater, Plasmonic nanoparticle enhanced light absorption in GaAs solar cells, Appl. Phys. Lett. 93 (2008) (121904–121904-3).
[7] Y. Ekinci, H.H. Solak, J.F. Löffler, Plasmon resonances of aluminum nanoparticles and nanorods, J. Appl. Phys. 104 (2008) (083107–083107-6).
[8] C. Langhammer, M. Schwind, B. Kasemo, I. Zoric, Localized surface plasmon resonances in aluminum nanodisks, Nano Lett. 8 (2008) 1461–1471.
[9] S.J. Tan, L. Zhang, D. Zhu, X.M. Goh, Y.M. Wang, K. Kumar, C.-W. Qiu, J.K.W. Yang, Plasmonic color palettes for photorealistic printing with aluminum nanostructures, Nano Lett. 14 (2014) 4023–4029.
[10] J. Olson, A. Manjavacas, L. Liub, W.,-S. Changa, B. Foerstera, N.S. King, M.W. Knight, P. Nordlander, N.J. Halas, S. Link, Vivid, full-color aluminum plasmonic pixels, PNAS 111 (2014) 14348–14353.
[11] M.W. Knight, L. Liu, Y. Wang, L. Brown, S. Mukherjee, N.S. King, H.O. Everitt, P. Nordlander, N.J. Halas, Aluminum plasmonic nanoantennas, Nano Lett. 12 (2012) 6000–6004.
[12] T.L. Temple, D.M. Bagnall, Optical properties of gold and aluminium nanoparticles for silicon solar cell applications, J. Appl. Phys. 109 (2011) 084343.
[13] P. Tassin, T. Koschny, M. Kafesaki, C.M. Soukoulis, A comparison of graphene, superconductors and metals as conductors for metamaterials and plasmonics, Nat. Photonics 6 (2012) 259–264.
[14] Y.A. Akimov, W.S. Koh, Design of plasmonic nanoparticles for efficient subwavelength light trapping in thin-film solar cells, Plasmonics 6 (2011) 155–161.
[15] U. Kreibig, M. Vollmer, Optical Properties of Metal Clusters, Springer, Berlin, 1995.
[16] H. Haberland, M. Karrais, M. Mall, Y. Thurner, Thin films from energetic cluster impact: a feasibility study, J. Vac. Sci. Technol. A 10 (1992) 3266–3272.
[17] H. Haberland, M. Mail, M. Mossier, Y. Qiang, T. Reiners, Y. Thurner, Filling of micron-sized contact holes with copper by energetic cluster impact, J. Vac. Sci. Technol. A 12 (1994) 2925–2930.
[18] K.J. Berg, A. Berger, H. Hofmeister, Small silver particles in glass surface layers produced by sodium-silver ion exchange - their concentration and size depth profile, Z. Phys. D 20 (1991) 309–311.
[19] H. Ehrenreich, H.R. Philipp, B. Segall, Optical properties of aluminum, Phys. Rev. 132 (1963) 1918–1928.
[20] L. Genzel, T.P. Martin, U. Kreibig, Dielectric function and plasma resonances of small metal particles, Z. Phys. B 21 (1975) 339–346.
[21] J.A. Scholl, A.L. Koh, J.A. Dionne, Quantum plasmon resonances of individual metallic nanoparticles, Nature 483 (2012) 421–427.